

Purification and Quality Control of Recombinant Septin Complexes for Cell-Free Reconstitution

Castro-Linares, Gerard; Den Haan, Jeffrey; Iv, Francois; Martins, Carla Silva; Bertin, Aurélie; Mavrakis, Manos; Koenderink, Gijsje H.

DOI

[10.3791/63871](https://doi.org/10.3791/63871)

Publication date

2022

Document Version

Final published version

Published in

Journal of Visualized Experiments

Citation (APA)

Castro-Linares, G., Den Haan, J., Iv, F., Martins, C. S., Bertin, A., Mavrakis, M., & Koenderink, G. H. (2022). Purification and Quality Control of Recombinant Septin Complexes for Cell-Free Reconstitution. *Journal of Visualized Experiments*, 2022(184), Article e63871. <https://doi.org/10.3791/63871>

Important note

To cite this publication, please use the final published version (if applicable). Please check the document version above.

Copyright

Other than for strictly personal use, it is not permitted to download, forward or distribute the text or part of it, without the consent of the author(s) and/or copyright holder(s), unless the work is under an open content license such as Creative Commons.

Takedown policy

Please contact us and provide details if you believe this document breaches copyrights. We will remove access to the work immediately and investigate your claim.

Purification and Quality Control of Recombinant Septin Complexes for Cell-Free Reconstitution

Gerard Castro-linares¹, Jeffrey den Haan¹, Francois Iv², Carla Silva Martins², Aurélie Bertin³, Manos Mavrakis², Gijsje H. Koenderink¹

¹ Department of Bionanoscience, Kavli Institute of Nanoscience Delft, Delft University of Technology ² Institut Fresnel, CNRS UMR7249, Aix Marseille Univ, Centrale Marseille ³ Institut Curie, Université PSL, Sorbonne Université

Corresponding Authors

Aurélie Bertin

Aurelie.Bertin@curie.fr

Manos Mavrakis

manos.mavrakis@fresnel.fr

Gijsje H. Koenderink

G.H.Koenderink@tudelft.nl

Citation

Castro-linares, G., den Haan, J., Iv, F., Silva Martins, C., Bertin, A., Mavrakis, M., Koenderink, G.H. Purification and Quality Control of Recombinant Septin Complexes for Cell-Free Reconstitution. *J. Vis. Exp.* (184), e63871, doi:10.3791/63871 (2022).

Date Published

June 23, 2022

DOI

10.3791/63871

URL

jove.com/video/63871

Introduction

The cytoskeleton has been classically described as a three-component system consisting of actin filaments, microtubules, and intermediate filaments¹, but recently, septins have been acknowledged as a fourth component

of the cytoskeleton¹. Septins are a family of GTP-binding proteins that are conserved in eukaryotes². Septins are involved in many cellular functions such as cell division³, cell-cell adhesion⁴, cell motility⁵, morphogenesis⁶, cellular

Abstract

Septins are a family of conserved eukaryotic GTP-binding proteins that can form cytoskeletal filaments and higher-order structures from hetero-oligomeric complexes. They interact with other cytoskeletal components and the cell membrane to participate in important cellular functions such as migration and cell division. Due to the complexity of septins' many interactions, the large number of septin genes (13 in humans), and the ability of septins to form hetero-oligomeric complexes with different subunit compositions, cell-free reconstitution is a vital strategy to understand the basics of septin biology. The present paper first describes a method to purify recombinant septins in their hetero-oligomeric form using a two-step affinity chromatography approach. Then, the process of quality control used to check for the purity and integrity of the septin complexes is detailed. This process combines native and denaturing gel electrophoresis, negative stain electron microscopy, and interferometric scattering microscopy. Finally, a description of the process to check for the polymerization ability of septin complexes using negative stain electron microscopy and fluorescent microscopy is given. This demonstrates that it is possible to produce high-quality human septin hexamers and octamers containing different isoforms of septin_9, as well as *Drosophila* septin hexamers.

infection⁷, and the establishment and maintenance of cell polarity⁸. Despite their important functions, how septins are involved in such processes is poorly understood.

The septin family of proteins is subdivided into several subgroups (four or seven, depending on the classification) based on protein sequence similarity². Members of different subfamilies can form palindromic hetero-oligomeric complexes, which are the building blocks of filaments and which, in turn, assemble into higher-order structures such as bundles, rings, and meshworks^{1,9,10,11,12}. Further molecular complexity arises from the presence of different splice variants, an example being human SEPT9, where there is evidence for specific functions of different splice variants^{13,14,15}. Additionally, the length of the hetero-oligomers depends on species and cell type. For instance, *Caenorhabditis elegans* septins form tetramers¹⁶, *Drosophila melanogaster* septins form hexamers¹⁷ (**Figure 1A**), *Saccharomyces cerevisiae* septins form octamers¹⁸, and human septins form both hexamers and octamers¹⁹ (**Figure 1A**). The ability of septin isoforms, splice variants, and post-translationally modified septins from the same subfamily to substitute each other in the complex and the (co-)existence of differently sized hetero-oligomers have made it difficult to delineate the cellular functions of different hetero-oligomeric complexes¹².

Another interesting ability of septins is their ability to interact with many binding partners in the cell. Septins bind the plasma membrane and membranous organelles during interphase and cell division^{20,21,22}. In dividing cells, septins cooperate with anillin^{23,24,25} and actin and myosin during cytokinesis^{26,27}. At the late stages of cytokinesis, septins seem to regulate the endosomal sorting complexes required for the transport (ESCRT) system for midbody abscission²⁸.

Additionally, there is also evidence of septin located on the actin cortex and actin stress fibers of cells in interphase cells^{29,30,31}. In specific cell types, septins also bind and regulate the microtubule cytoskeleton^{32,33}.

All of these features make septins a very interesting protein system to study, but also a challenging one. The combination of the large number of septin subunits (13 genes in humans without counting splice variants²) with the potential of septin subunits from the same subfamily to substitute each other and form differently sized hetero-oligomers makes it difficult to draw a conclusion on the cellular function of a specific septin by genetic manipulation. Furthermore, the multiple interactions of septins make interpreting the effects of common research tools such as drugs³⁴ directed at cytoskeletal or membrane components a hard task.

A way to overcome this situation is to complement research in cells with *in vitro* (cell-free) reconstitution of septins. *In vitro* reconstitution allows for the isolation of a single type of septin hetero-oligomers with a specific subunit composition and length^{18,35,36,37}. This complex can then be studied in a controlled environment, either alone to discover the basic structural and physicochemical properties of septins^{38,39,40}, or in combination with desired partners such as model biomembranes^{11,41,42}, actin filaments^{10,27}, or microtubules^{32,36} to decipher the nature of their interactions.

Therefore, a reliable method to purify different septin complexes efficiently is vital for septin research. However, even using the same protocol, different purifications can give proteins with different activity/functionality or even integrity. For commercially available proteins such as enzymes, the functionality and enzymatic activity are carefully validated⁴³. Implementing careful quality control for cytoskeletal or

structural proteins such as septins can be challenging, but it is essential to make experiments across labs comparable.

This paper describes a robust method to purify high-quality recombinant septins in their hetero-oligomeric form based on the simultaneous expression of two vectors containing mono- or bi-cistronic constructs (**Table 1**) in *Escherichia coli* cells. The method consists of a two-step affinity chromatography approach to capture septin hetero-oligomers containing both a his₆-tagged septin and a Strep-II-tagged septin (**Figure 1B,C**). This protocol, first described in Iv et al.¹⁰, has been used to purify *Drosophila* septin hexamers^{11,27,35}, human septin hexamers¹⁰, and several human septin octamers containing different native (isoform 1, 3, and 5)^{10,32} or

mutated SEPT9 isoforms³². Furthermore, a description of a set of techniques to assess the quality of the purified septins is given. First, the integrity and correct stoichiometry of the septin subunits is checked using denaturing electrophoresis and transmission electron microscopy (TEM). Then, the presence of hetero-oligomers of the correct molecular mass and the presence of monomers or smaller oligomers indicative of complex instability are examined by native electrophoresis and mass photometry via interferometric scattering microscopy (iSCAT). Finally, the last step consists of the assessment of the polymerizing activity of the septins using fluorescence microscopy and TEM.

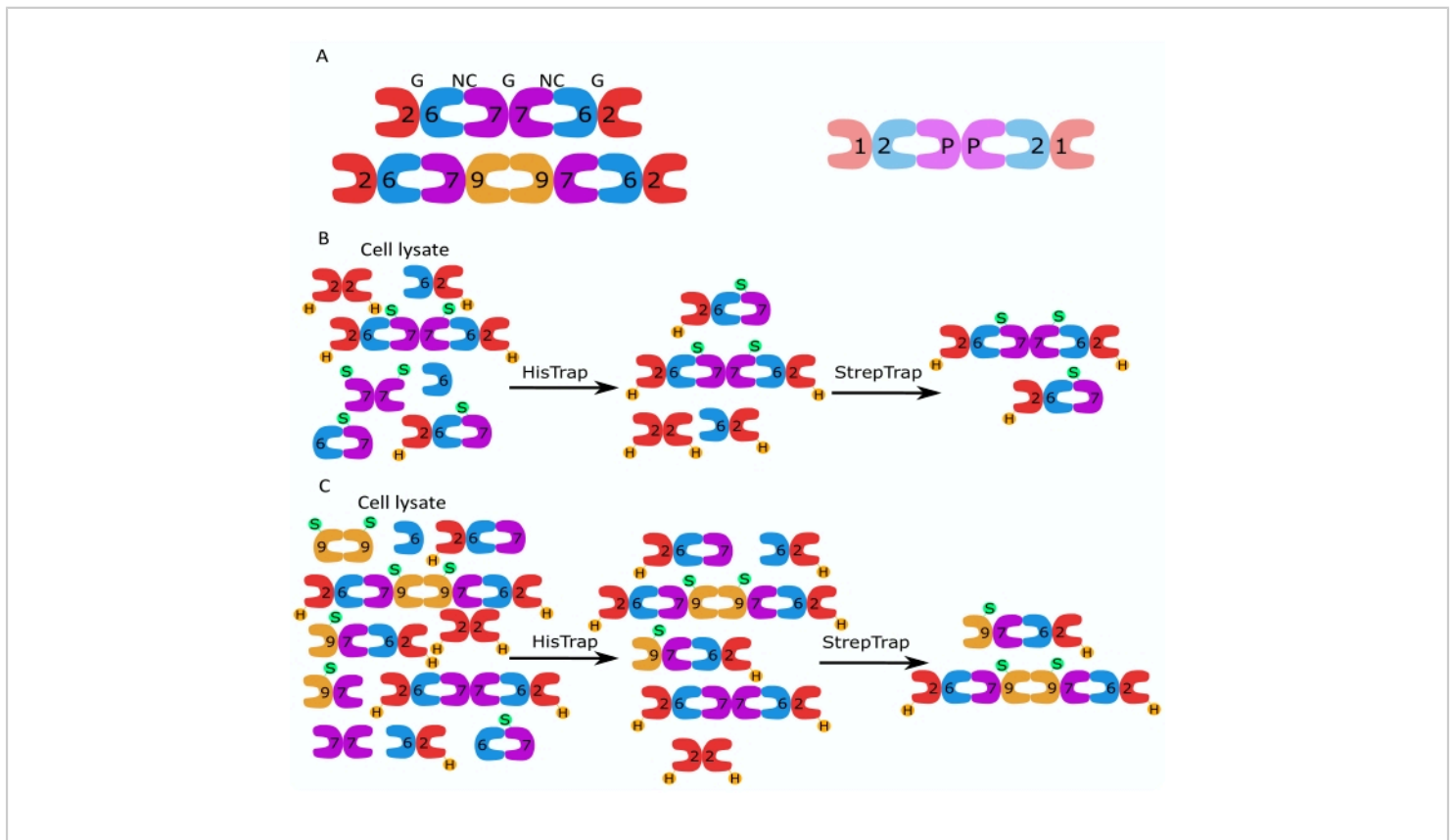


Figure 1: Purification strategy. (A) Schematics of the septin hetero-oligomers that exist in human (left) and *Drosophila* (right) cells. Numbers denote septin subunits from the indicated groups, and P denotes Peanut. Human SEPT9 can be any of its isoforms. The septin subunits have an asymmetric shape and are longitudinally associated with two distinct interfaces,

the NC:NC and the G:G interface, as denoted by NC and G, respectively, on top of the human hexamer. **(B,C)** Schematic illustration of the two-step chromatography strategy, shown for **(B)** human septin hexamers and **(C)** octamers. H indicates the his-tags, while S indicates the Strep-II-tags. [Please click here to view a larger version of this figure.](#)

Protocol

1. Purification of septin hetero-oligomers

1. Co-transformation of bacterial cells with the expression vectors

1. Select a combination of one pnEA and one pnCS plasmid⁴⁴ that will be used for expression. Choose the combination depending on the desired subunit composition of the septin hetero-oligomer^{10,35} and on whether or not fluorescent tagging is required.

NOTE: C-terminally tagged monomeric superfolder GFP (msfGFP)-tagged SEPT2 (for human septins) or msfGFP- or monomeric enhanced GFP (mEGFP)-D Sep2 (for *Drosophila* septins) is used here (**Table 1**).

2. Pipette 1 μL of each plasmid ($\sim 1 \text{ ng}/\mu\text{L}$) into 100 μL of competent BL21 *Escherichia coli* cells and incubate on ice for 20 min.
3. Place the cells in a water bath at 42 °C for 40 s and then immediately incubate them for 3 min on ice.
4. Add 0.9 mL of lysogeny broth (LB) medium to the cell suspension and let the cells grow for 1 h at 37 °C. Plate 100 μL of cells on warm LB-agar plates containing 100 $\mu\text{g}/\text{mL}$ ampicillin and 100 $\mu\text{g}/\text{mL}$ spectinomycin and incubate overnight at 37 °C.

2. Grow bacterial pre-culture

1. Fill a 250 mL Erlenmeyer flask with 100 mL of Terrific broth (TB) or LB medium containing 100 $\mu\text{g}/\text{mL}$ ampicillin and 100 $\mu\text{g}/\text{mL}$ spectinomycin.
2. Pick out a single colony from the LB-agar plate with a sterile inoculation loop and transfer it to fresh media from step 1.2.1.
3. Incubate at 37 °C in a rotary shaker incubator, either overnight or for at least 6 h.

NOTE: From this culture, a glycerol stock can be prepared by mixing the bacterial suspension 1:1 with glycerol and stored at $-80 \text{ }^\circ\text{C}$. This stock can be used in step 1.2.2. instead of a freshly transformed colony.

3. Bacterial culture and protein expression induction

1. Transfer 100 mL of grown bacteria into 5 L of TB or LB containing 50 $\mu\text{g}/\text{mL}$ ampicillin and 50 $\mu\text{g}/\text{mL}$ spectinomycin.
2. Grow this culture at 37 °C in a shaker incubator until it reaches an optical density (OD) measured at a wavelength of 600 nm in the range of 2-3 for unlabeled septins or 0.6-0.8 for msfGFP/mEGFP-labelled septins and induce protein expression by adding a final concentration of 0.5 mM IPTG. The lower OD for the labeled septins is to avoid reaching the death phase in their longer expression time, as detailed in the next step.
3. Incubate the cells expressing unlabeled septin hetero-oligomers for 3 h at 37 °C or the

cells expressing msfGFP-labelled hetero-oligomers overnight at 17 °C.

NOTE: The short protein expression time for unlabeled complexes, facilitated by the use of the richer TB medium, is chosen to prevent protein degradation. The longer expression time combined with lower temperature for labeled complexes is chosen to allow for correct folding of the msfGFP tag.

4. Bacterial lysis and lysate clarification

NOTE: From this point onwards in the purification procedure, keep the protein-containing solution on ice or at 4 °C at all times to prevent proteolytic protein degradation or loss of activity.

1. Collect the cultured cells by centrifuging at 4,000 x g for 20 min at 4 °C. Discard the supernatant.
 1. Optionally, snap-freeze the pellet in this step and store at -80 °C for maximally 6 months. If this option is chosen, make sure to thaw the pellet on ice before continuing.
2. Dissolve the pellet in 100 mL of lysis buffer (**Table 2**) and lyse the cells. Choose one of the two options below
 1. Sonicate in 7 cycles of 30 s ON and 59 s OFF with a tip sonicator using 30% amplitude (note that the settings are sonicator-dependent).
 2. Break down the cells in the French press by passing them at least 3x.
3. Clarify the cell lysate by centrifuging at 20,000 x g for 30 min at 4 °C and keep the supernatant. It is recommended to start with step 1.5.1. during this centrifugal step.

4. Optionally, take a sample for denaturing electrophoresis, as described in section 2.

5. Affinity chromatography for His-tagged proteins

NOTE: This step yields complexes containing human SEPT2 or *Drosophila* Sep1 using a nickel column (**Figure 1B**).

1. Equilibrate a pre-packed nickel sepharose high-performance chromatography column with septin buffer (**Table 2**).
2. Load the clarified supernatant onto the column at 1 mL/min and wash the bound protein with at least three column volumes of septin buffer.
3. Elute the septin complexes with 50% HisTrap elution buffer (**Table 2**) at 1 mL/min while collecting 0.5 mL fractions to yield an imidazole concentration of 250 mM.
4. Pick the fractions containing septin complexes, as indicated by the optical absorbance of the eluate at 280 nm monitored online with a fast protein liquid chromatography (FPLC) system or after the purification with a microvolume spectrophotometer.

NOTE: Imidazole absorbs light at 280 nm. This probably explains why the protein peak does not go back to zero absorbance after the septin elution (**Figure 2A**).

6. Affinity chromatography for Strep-II-tagged proteins

NOTE: This step yields complexes containing either human SEPT7 (hexamers), human SEPT9 (octamers), or *Drosophila* peanut using a Strep-Tactin column (**Figure 1B**). The chromatography column is based on a modified biotin-streptavidin system. The protein is tagged with modified biotin (Strep-II-tag), and the column contains an engineered streptavidin (Strep-Tactin).

Despite being modified from the biotin-streptavidin system, there is no interference between the Strep-Tactin-Strep-II-tag system and the biotin-streptavidin system. The described system is used to avoid interference with reconstitution assays using biotin and streptavidin.

1. Equilibrate a pre-packed StrepTactin sepharose high-performance chromatography column with septin buffer (**Table 2**). Load the septin-containing fractions recovered from the nickel column at 1 mL/min and wash the bound protein with at least three column volumes of septin buffer.

2. Elute the septin complexes with 100% StrepTrap elution buffer (**Table 2**) at 1 mL/min while collecting 0.5 mL fractions to yield a concentration of 2.5mM desthiobiotin.

NOTE: The desthiobiotin in the StrepTrap elution buffer must be dissolved fresh.

3. Pick the fractions containing septin complexes, as indicated by the optical absorbance of the eluate at 280 nm monitored online with an FPLC system or after the purification with a microvolume spectrophotometer.

NOTE: The denaturing electrophoresis is usually done at this point with samples of the column washings and septin fractions. The order of columns can be inverted with indistinguishable results, i.e., the clarified lysate after step 1.4. can be subjected to Strep-Tactin affinity chromatography followed by nickel affinity chromatography.

7. Dialysis and storage

1. To remove the desthiobiotin from the final storage solution, dialyze the septin complexes in a ~1:300

sample-to-buffer volume ratio against septin buffer (**Table 2**) supplemented with 1 mM DTT overnight, or for at least 4 h, at 4 °C using a 30 kDa MWCO dialysis membrane.

2. Optionally, concentrate the septins using a 30 kDa MWCO centrifugal concentration column up to the desired concentration. Aim for a concentration of 5-7 μM, as measured via the solution optical absorbance at 280 nm and using a theoretical extinction coefficient calculated via ProtParam (**Table 3**).

3. Aliquot the protein complexes into the desired aliquot size, snap-freeze the aliquot, and store it at -80 °C.

NOTE: It is recommended not to store the protein for more than 6 months. In addition, it is recommended to perform regular quality control experiments, especially if the protein is stored for longer than the recommended time.

2. Quality control of purity and integrity of the septin hetero-oligomer

NOTE: The hetero-oligomer quality control consists of a set of biochemical and imaging techniques that allow for the detection of the mass and integrity of the septin complexes present in the solution.

1. Denaturing electrophoresis to check for the formation of the septin hetero-oligomer with the correct components

1. Mix 10 μL of the selected fractions with 10 μL of 2x SDS sample buffer, load them onto a precast 4%-15% TGX gel, and fill the system with Tris/glycine/SDS running buffer.

2. Run the electrophoresis for 35 min at 200 V and stain the gel (**Table of Materials**) to visualize the results.

The molecular weights of the individual septin proteins and septin hetero-oligomeric complexes can be found in **Table 3**.

3. Measure the relative intensity of each band inside each lane containing purified septins in a contrast-inverted image. Do this by calculating the mean intensity of equally sized rectangles around each band and of an equally sized rectangle on a region without any band in the same lane. Then, normalize the values by dividing the intensity of each band by the intensity of the region without bands.

NOTE: If the intensity is saturated (for example, values of 255 for an 8-bit image on a contrast-inverted image), skip the lane.

2. Ensemble-averaged native size distribution *via* native electrophoresis

1. Prepare 800 mL of anode buffer and 200 mL of light blue cathode buffer the day before and store them in the fridge. To prepare the anode buffer, dilute 40 mL of 20x running buffer with 760 mL of type-I deionized water (I-water). To prepare the light blue cathode buffer, dilute 10 mL of 20x running buffer and 1 mL of 20x cathode additive with 189 mL of I-water. The running buffer and cathode additive come with a kit (**Table of Materials**).
2. Prepare 10 μ L of the sample by mixing ~500 ng of septin with the needed amount of sample buffer (2.5 μ L in this case, due to the use of a 4x sample buffer; see **Table of Materials**) and enough I-water to reach a volume of 10 μ L.
3. Load the samples onto the gel and fill the system with the ice-cold anode and cathode buffers.

4. Run the electrophoresis for around 115 min at 150 V with a power supply that does not stop at low currents and stain the gel (**Table of Materials**) to visualize the results. The molecular weights of the single proteins and complexes calculated based on the sequence can be found in **Table 3**.

3. Single-molecule mass distribution using mass photometry via interferometric scattering microscopy

1. Wash #1.5 glass slides by sonicating them in an ultrasonic cleaner for 5 min in I-water, 5 min in isopropanol, and finally, 5 min in I-water.
2. Dry two glass slides with a gentle stream of nitrogen gas and place a 7 μ L drop of 0.01% Poly-L-Lysine (PLL) solution on the center of one of the slides. Then, place the center of the other slide on top of the PLL drop, orienting the two slides orthogonally for easy separation. Incubate for 30 s.

1. Wash by immersing in a beaker with I-water 1x and by directly applying a stream of I-water 2x. Then, dry the two slides with a flow of nitrogen gas. These slides can be stored afterward for around 6 weeks at room temperature in dry conditions.

NOTE: Label the side of the slide that is treated with the PLL-PEG to correctly run the experiment.

3. Just before the experiment, cut a piece of 2 x 2, 3 x 2, or 3 x 3 gaskets (that yield 4, 6, or 9 imaging chambers/slide, respectively) and stick it on the PLL-PEG-treated part of a glass slide while avoiding the glass slide and the gaskets contacting any dirty surface. Place the slide on a light-duty wiper tissue

and press on the gaskets with a pipette tip to stick them with the protecting plastic still on the gaskets.

4. Warm septin buffer (**Table 2**) to room temperature and thaw the proteins in hand (keep them on ice afterward).

NOTE: iSCAT shows the signal of some detergents and small molecules that resemble protein signals⁴⁵. DTT is one of those small molecules, and that is why it is not used for this experiment. There is only a trace of DTT coming from the stored septin.

5. Place the slide with gaskets on the commercial mass photometry system containing 19 μL of septin buffer and focus the microscope using the autofocus option. Follow the manufacturer's instructions to check if the found focus is correct.

1. Optimize the frame rate and the exposure time by pressing on **Optimize illumination** and refocus with the autofocus option with the new settings. The standard 100x objective that is part of the setup is used here.

6. Create or load a project folder to store the data using **File > New Project or File > Load Project**.

7. Pipette 1 μL of sample onto the 19 μL of septin buffer drop (step 2.3.5) used to focus and mix while minimizing the movement of the slide by not touching anything while doing so. Then, record a 6,000-frame video by clicking on **Record**.

1. For correct analysis, record the following samples: septin buffer, protein mass standard for the calibration of the signal-to-mass ratio (if a recent calibration is available and the environmental conditions have not changed, this sample can be skipped), and 250 nM of

septin complexes diluted in septin buffer without DTT (this gives a final concentration of ~ 12.5 nM).

8. Analyze the videos using the manufacturer's software to obtain the protein mass distribution. Check for good quality data as follows.

1. If the peaks of different septin hetero-oligomers sizes are overlapping too much or too many events are detected ($>3,500$ events for a 6,000-frames video with the regular field of view of 128 pixels x 34 pixels spanning 10.8 μm x 2.9 μm), decrease the final septin concentration and measure again.
2. If there are not enough counts of single molecules measured (at least 2,500-3,500 for a 6,000-frame video with the regular field of view), increase the septin concentration and measure again.

4. Direct imaging of septin complexes via negative stain transmission electron microscopy

1. Dilute samples to a concentration of about 50 nM in septin buffer and prepare the staining solution (2% uranyl formate or uranyl acetate in I-water).

NOTE: Uranyl formate must be prepared fresh.

2. Pipette 4 μL of diluted septins onto a glow discharged electron microscopy grid and incubate for 30 s.
3. Remove most of the protein solution using a filter paper and wash the grid 2x with septin buffer and 1x with I-water to remove loosely adsorbed septins.
4. Stain with 2% uranyl acetate or uranyl formate solution in I-water for 1 min, absorb the staining

solution with a filter paper, and air-dry the grid for a few minutes.

5. Screen the grid using a properly aligned transmission electron microscope to search for regions of enhanced stain and collect about 100 images within these selected areas.
6. Collect images at a magnification of at least 50,000x to obtain a pixel size of about 2 Å/pixel and with a defocus varying from $-1\ \mu\text{m}$ to $-2\ \mu\text{m}$. Use an acceleration voltage of 200 kV. Preferably, use an automated procedure to collect the data, which will depend on the acquisition software available.
7. Perform 2D image processing using dedicated software
 1. Box out at least 2,000 particles using a dedicated software⁴⁶.
 2. Perform two-dimensional alignment and classification iteratively until classes are obtained without further improvement. The first alignment and classification step should be reference-free to avoid any bias in the classification.
 3. Use the averages obtained from the first reference-free classification as new references to carry out an extra round of classification. Repeat this process iteratively until no further improvement is achieved. Ensure that each class is based on 50 to 100 picked particles, and individual subunits are clearly visible. Different software tools can be used (Spider, Eman, or Relion)^{46,47,48}.

3. Septin functional quality control via polymerization analysis

NOTE: The functionality quality control consists of a set of imaging techniques that allow for the detection of polymerized septin complexes. Below, unlabelled septins are referred to as "dark" septins, and the buffer used for polymerizing unlabelled septins is referred to as "dark" septin polymerization buffer (SPB).

1. Septin bundle imaging via fluorescence microscopy
 1. Prepare the 5x fluoSPB (**Table 2**) and a septin mix consisting of 90% dark septin and 10% msfGFP-septin at six times higher concentration than the desired final concentration in septin buffer + 1 mM DTT. A typical concentration for this assay is 300 nM, and, therefore, the concentration is 1,800 nM for this mix.
 2. Polymerize the septin by mixing, in this specific order, I-water (enough to top up to the final desired volume), 20% 5xfluoSPB (a final dilution of 1:5), 0.05 μM PCD, and 16.67% septin mix (a final dilution of 1:6). For 10 μL , mix 6.23 μL of I-water, 2 μL of 5xfluoSPB, 0.1 μL of PCD (with a stock of 5 μM), and 1.67 μL of septin mix. Incubate this mix for at least 30 min at room temperature.
 3. Add the samples to an imaging chamber washed with fluoSPB (**Table 2**) and image the septin bundles. PLL-PEG-passivated flow channels, as described in previous research^{10,32}, work well for this experiment.
2. Septin bundle imaging via negative stain transmission electron microscopy

1. Prepare the 5x darkSPB (**Table 2**) and a septin mix consisting of 100% dark septin at six times higher concentration than the desired final concentration in septin buffer + 1 mM DTT. A typical concentration for this assay is 300 nM, and, therefore, the concentration is 1,800 nM for this mix.
2. Polymerize the septin complexes by mixing, in this specific order, I-water (enough to top up to the final desired volume), 20% 5xdarkSPB, and 16.67% septin mix. For 5 μ L, mix 3.16 μ L of I-water, 1 μ L of 5x darkSPB, and 0.83 μ L of septin mix. Incubate this mix for at least 30 min at room temperature.
3. Add 3-5 μ L of sample to a glow-discharged electron microscopy grid and incubate for 1 min. Then, wash the grid 2x with darkSPB (**Table 2**) by absorbing the liquid with a filter paper and adding a drop of darkSPB buffer, wash 1x with I-water, incubate for ~30 s with 2% uranyl acetate, blot the stain, and air-dry the sample for a few minutes.
4. Image the septin bundles at 120 kV and magnifications between 5,000x and 60,000x with a defocus of between 1-2 μ m.

Representative Results

As mentioned in the protocol, 5 L of *E. coli* cells co-transformed with the two septin-expressing plasmids were grown, and the expression of septins was induced by adding IPTG. After 3 h, the cells were collected by centrifugation, resuspended in lysis buffer, and lysed by sonication. The lysate was then clarified by centrifugation, and the clarified solution was applied to a HisTrap column (**Figure 2A**). After the first purification, the septin-containing fractions were

pooled and applied onto a StrepTrap column (**Figure 2B**). This typically yields around 3-5 mL of ~1 μ M septin complex. Before pooling the septin-containing fractions, denaturing gel electrophoresis can be used to check for the integrity of the septin subunits and the equimolar stoichiometric ratio between the different septin subunits forming the complex. (**Figure 3A**). If the gel shows similarly intense bands corresponding to the molecular weights (**Table 3**) of the septin subunits, the protocol can be continued. If not, it is recommended to start the protocol again. In the example shown for human septin octamer with SEPT9_i1, **Figure 3A** clearly shows bands corresponding to SEPT9_i1, SEPT6, SEPT7, and SEPT2 (in the order from top to bottom) with similar intensities; the 99% confidence interval of the normalized intensity was 1.128 ± 0.048 for SEPT2, 1.092 ± 0.034 for SEPT6, 1.108 ± 0.040 for SEPT7, and 1.067 ± 0.029 for SEPT9. If SEPT2 is tagged with msfGFP, it will shift up very close below SEPT9_i1. Depending on the electrophoresis system used and the presence of the C-terminal TEV-Strep tag for SEPT7 (which makes it migrate more slowly than untagged SEPT7), the SEPT7 and SEPT6 bands sometimes merge due to their comparable molecular weights. The next step is to pool the fractions and dialyze them against septin buffer with DTT. After the dialysis, if the concentration is too low (<2 μ M) or a higher concentration is needed for the experiments, a concentration step can be included, as described in the protocol. Concentrations below 1 μ M usually indicate a bad functional quality of the septins. A final septin complex concentration between 3.5 μ M and 7 μ M works well for most *in vitro* assays. These concentrations are usually obtained when the volume after concentration reaches 0.5-1 mL.

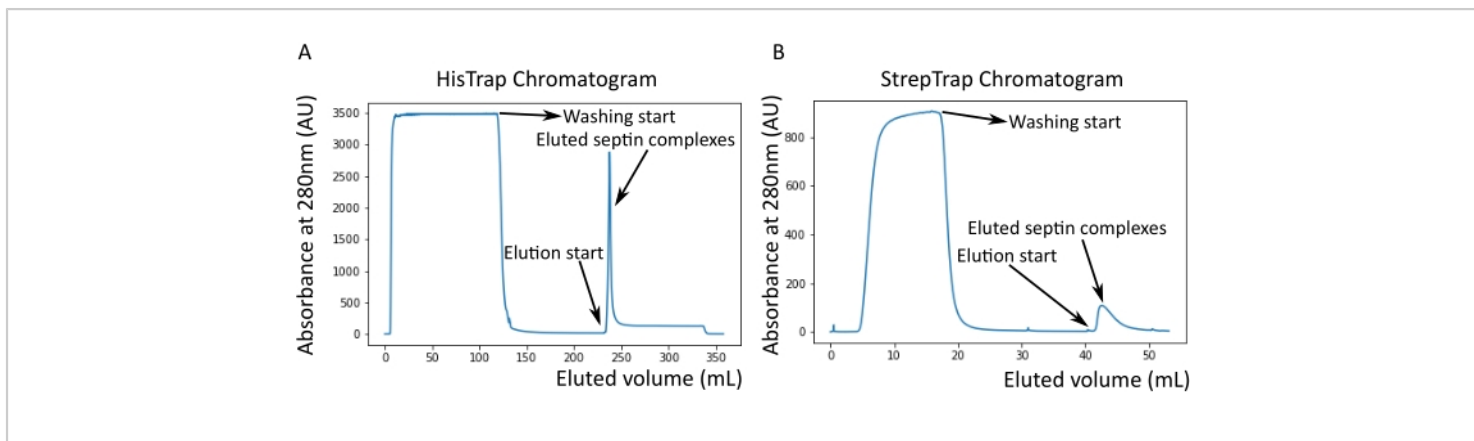


Figure 2: Example chromatograms corresponding to the purification of dark human septin octamers_9i1. (A) HisTrap column chromatogram. After the septin elution peak, the absorbance does not go back to zero, likely due to the presence of imidazole in the buffer. The pooled fraction went from the start of the elution peak until the absorbance stabilized at around 250 mL. (B) StrepTrap column chromatogram. The pooled fraction went from the start of the elution peak until the absorbance went back to around 0 at 50 mL. [Please click here to view a larger version of this figure.](#)

To continue with the quality control, native electrophoresis, as described in the protocol, was performed (Figure 3B). In the gels, a major band corresponding to the intact heterooligomers and, usually, a minor band corresponding to dimers can be observed. Human hexamers are found a little bit above the 242 kDa marker band, while octamers are found above the 480 kDa band, above their calculated molecular mass. The location of these bands was checked by western blot analysis of eukaryotic cell extracts³². Tagging with msfGFP couples each SEPT2 with an msfGFP protein. This causes an increase in the molecular weight of septin complexes of 53.4 kDa (26.7 kDa/msfGFP molecule). Nevertheless, on the native electrophoresis gel, the apparent molecular weight of the msfGFP-tagged complexes is indistinguishable from that of the untagged complexes.

A complementary technique to test whether the septin complexes are intact is mass photometry by iSCAT microscopy. iSCAT monitors the light scattering of molecules

landing on a glass slide amplified by interference with reference light, typically the reflection of the laser on the bottom of the glass slide. Then, a background subtraction approach is used to give contrast to the particles. Due to this correction, the signal shows positive and negative values depending on whether the particles land on the glass or move away from it⁴⁹. The detected signal is directly proportional to the molecular weight of proteins⁵⁰. Therefore, a signal-to-mass calibration with a mass standard can determine the mass of the sample proteins. Figure 3C shows an example of human septin octamers containing SEPT9_i1. Most of the detected single particles (~50%) are of a molecular weight expected for complete octamers containing SEPT9_i1 (423 kDa) (Figure 3C). There are also particles with masses between 150-300 kDa, but no clear peak is observed, indicating the possible presence of other septin species in low abundance. Similarly, most of the detected single particles for mEGFP-tagged *Drosophila* hexamers are of a molecular weight expected for intact hexamers (361 kDa) (Figure 3D).

An additional clear peak at 241 kDa indicates the presence of stable tetramers containing two peanut proteins, one DSep1 and one mEGFP-DSep2. Finally, both the human and the fly septin complexes show a peak around 80 kDa that could be

a mix of monomers and dimers, possibly amplified by a trace of DTT or any other small molecule that aggregates, showing a peak in the positive side of the plot⁴⁵.

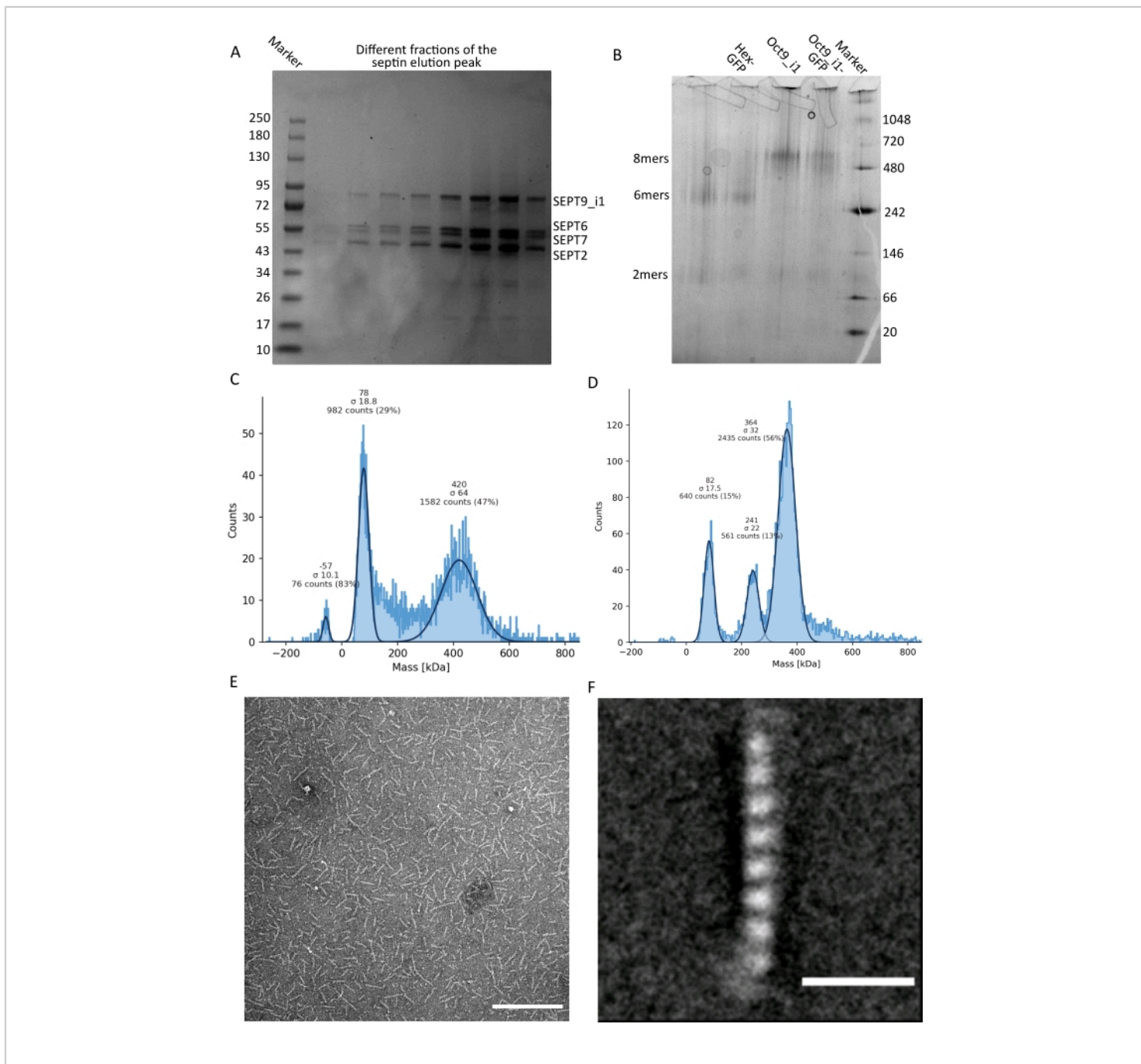


Figure 3: Examples of results of the oligomer quality control. (A) Example of denaturing gel showing different fractions of the elution peak from the purification of dark human septin octamers_9i1. (B) Example of native electrophoresis

of different septin complexes. **(C,D)** Different examples of histogram results of mass photometry at 12.5 nM of septin complexes: **(C)** dark human septin octamers_9i1 and **(D)** DSep1-msfGFP *Drosophila* septin hexamers. Lines are Gaussian fits. **(E)** TEM image of 25 nM dark human septin octamers_9i1 in septin buffer. Scale bar = 200 nm. **(F)** Class average image of SEPT2-msfGFP human septin octamers_9i1. The msfGFP tags are visible as fuzzy densities on the two ends. Scale bar = 10 nm. Panels **(E)** and **(F)** are the copyright of The Company of Biologists and have been adapted from Iv et al.¹⁰ with permission. [Please click here to view a larger version of this figure.](#)

Given that both native gels and iSCAT provide ensemble-averaged information only, class averaging of transmission electron microscopy images of single septin oligomers was used to check the integrity and purity of the complexes by direct visualization. In TEM images of septin complexes in septin buffer, rods of 24 nm (hexamers) or 32 nm (octamers) in length can be observed. An example of a human septin octamer containing SEPT9_i1 can be seen in **Figure 3E**. When class averaging them, each of the subunits can be observed and counted, as seen for the msfGFP-tagged human octamer with SEPT9_i1 in **Figure 3F**. In case the oligomer is fluorescently labeled, extra densities that correspond to the SEPT2-msfGFP can be observed at the end of the rods (**Figure 3F**).

The combination of the above techniques proves that octamers (or hexamers) with the correct stoichiometric ratio and high purity can be purified using the described protocol. Finally, the last quality control check is for the functionality of the septin complexes in terms of their polymerization ability. In the presence of low salt concentration (<150 mM KCl with the described buffer⁹), if septins are not in the presence of other proteins or negatively charged lipid membranes,

they self-assemble into bundles⁹. Septins are prevented from polymerization by keeping them in the storage buffer, which has a high (300 mM) KCl concentration. The septin hetero-oligomers are then diluted at a 1:6 volume ratio in a buffer of the same composition but without KCl to achieve a final KCl concentration of 50 mM. To do fluorescence imaging, this buffer is complemented with an oxygen scavenging system to protect from photobleaching and with a blinking suppressor. In TIRF microscopy, small clusters of proteins can be observed within the shallow TIRF field (~100 nm; **Figure 4A,B**). On a confocal microscope, large clusters of filamentous structures can be seen floating higher up in solution (**Figure 4C**). Finally, with TEM, small bundles of septin (**Figure 4D**), corresponding to the clusters observed by TIRF, and large bundles (**Figure 4E**), corresponding to the structures observed by confocal microscopy, can be observed. The insets of **Figure 4D,E** reveal that both types of structures consist of long, thin filaments that run in parallel, forming bundles with tapered ends. Together, the fluorescence and TEM images prove that the purified septin complexes can polymerize into filaments, which in turn self-assemble into bundles.

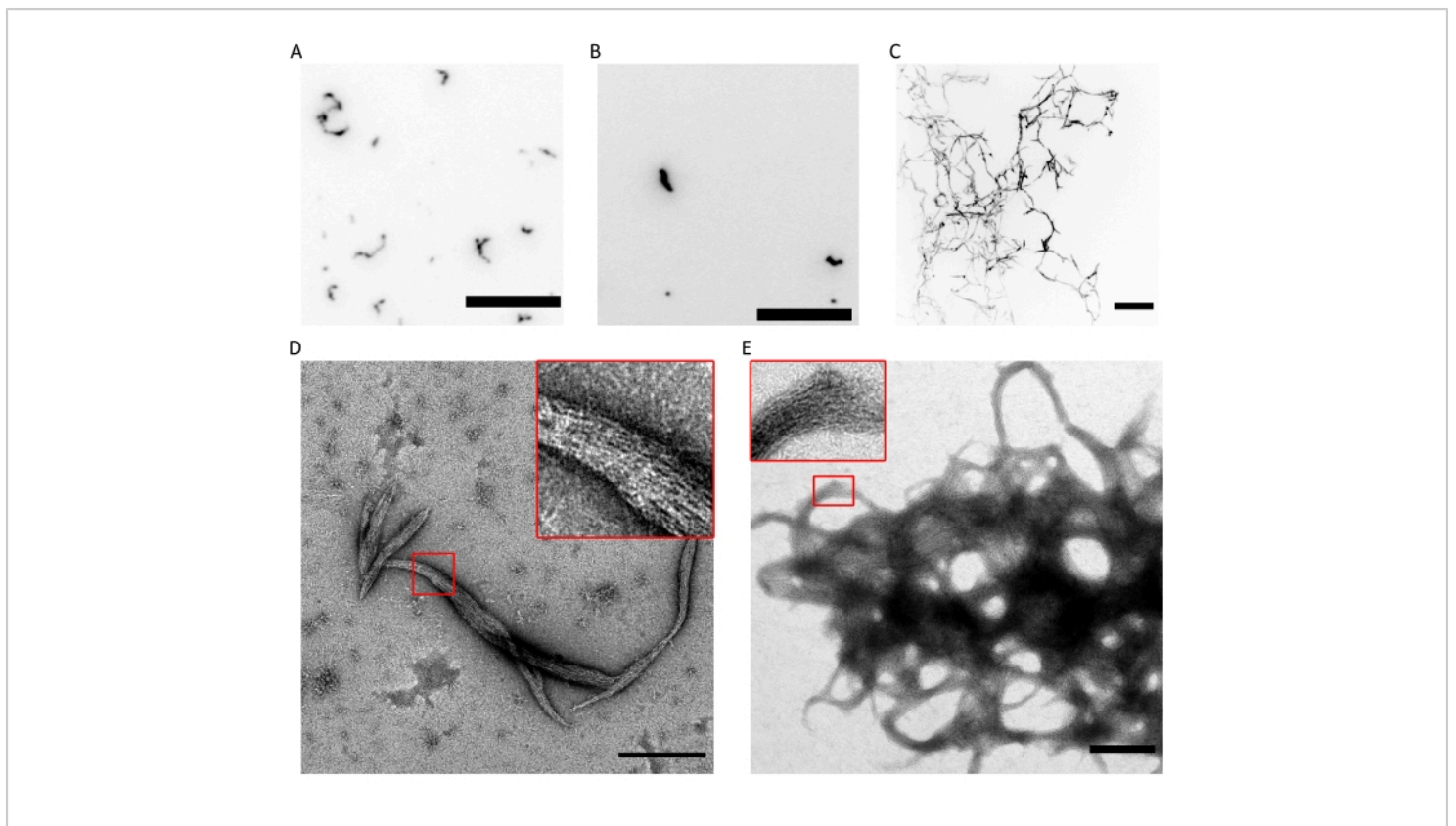


Figure 4: Examples of results of the polymerization ability quality control. (A) TIRF image of 300 nM human septin hexamers (10% msfGFP-labelled hexamers) in fluoSPB. (B) TIRF image of 300 nM human septin octamers containing SEPT9_i1 (10% msfGFP-labelled octamers9_i1) in fluoSPB. (C) Confocal maximum-intensity projections of Z-stacks across ~30 µm with 0.5 µm of spacing of 300 nM human septin octamers_9i3 in fluoSPB. (A-C) Scale bar = 10 µm and inverted grayscale. (D,E) Example TEM images of (D) small and (E) large bundles of human septin octamers_9i1 in darkSPB. Insets show regions where clear filaments running parallel within the bundle can be observed. Scale bars = 500 nm. Panels (C-E) are copyright of The Company of Biologists and have been adapted from Iv et al.¹⁰ with permission. [Please click here to view a larger version of this figure.](#)

Table 1: List of plasmids. Plasmids to purify septin oligomers following this protocol. All plasmids have been deposited in Addgene (first column). [Please click here to download this Table.](#)

Table 2: List of buffers. Buffer compositions used for the purification and quality control of septin oligomers. [Please click here to download this Table.](#)

Table 3: Molecular weights and extinction coefficients. List of molecular weights (MW) and optical extinction coefficients (ϵ) at a wavelength of 280 nm calculated with ProtParam based on the sequences of the complex, assuming linear fusion of the septin subunits, the different septin complexes, and the unique septin subunits (only MW)

that can be purified with the plasmids listed in **Table 1**. [Please click here to download this Table.](#)

Discussion

The method described here allows for the robust purification and quality control of pre-formed septin hetero-oligomers. Some of the key issues to consider for the correct application of the method are as follows. During the elution steps in the chromatographic separations, it is important to use the recommended (or lower) flow rate to minimize the dilution of the septin complexes. Additionally, to maximize the recovery of protein during the final concentration step, the concentrator column is oriented in such a way that the solution is not pushed against the filter (when there is only a filter on one side). If the solution goes directly to the filter, the protein sticks much more to it, substantially decreasing the final yield. It is also important to consider that the concentration step is not always necessary. Picking fractions only from a narrow range around the peak in the chromatogram usually gives a high enough stock concentration (>3,000 nM) for many reconstitution applications (which usually operate between 10-300 nM). Finally, for the quality control of the functionality of the septin complexes by fluorescence microscopy, it is important to correctly passivate the surface of the microscopy slides, since septin complexes avidly stick to glass. Passivation of the glass slides can be done either via PLL-PEG functionalization or by the formation of neutral (100% DOPC) supported lipid bilayers^{11,32}.

Compared to the original purification protocol first described in Iv et al.¹⁰, there is a change in the buffer compositions (**Table 2**). The concentration of MgCl₂ has been reduced from 5 mM to 2 mM, and the concentration and pH of Tris-HCl have been reduced from 50 mM to 20 mM and from 8.0 to 7.4, respectively. These changes were made to make the

buffer conditions compatible with studies of the interactions of human septins with lipid bilayers, actin filaments, and microtubules^{10,11,32}. This is because the authors formed supported lipid bilayers and polymerized actin in the F-buffer, whose composition is identical to that of darkSPB, apart from the presence of ATP in the F-buffer. The buffer change did not produce any changes in the quality or lifetime of the purified septins compared to the original buffers.

This method of purification still has several limitations. First, different purification attempts can vary in yield (0.5-1 mL of 2-5 μM septin complexes) and functional quality, as checked by the bundle formation ability of the purified septin complexes. That is why it is very important to consistently perform the quality checks described in this paper. Controlling very well the times of expression and the optical density of the bacterial culture can help mitigate the difference in yield. Second, this purification pipeline cannot distinguish between trimers and hexamers or between tetramers and octamers (**Figure 1B**). However, the quality control experiments can be used to prove that the majority of septin complexes are in their long oligomer form. In case an even narrower oligomer size distribution is required, size exclusion chromatography can be inserted in between step 1.6. and step 1.7. of the purification protocol. This optional step, however, dramatically decreases the yield, and it is not recommended unless it is strictly needed. A last, more fundamental, limitation comes from the use of *E. coli* as an expression system for recombinant septin complexes. Naturally, this system does not allow for post-translational modifications (PTMs), which have been reported in animal cells, such as phosphorylation, acetylation, and sumoylation^{6,51,52,53}. These posttranslational modifications could be added by implementing a similar purification strategy in insect or human cells. Furthermore, this paper has only discussed the reconstitution of septins by themselves,

but studies in cells indicate that regulatory proteins such as proteins from the Borg family^{54,55} and anillin^{24,25,56} can have substantial yet poorly understood effects on the assembly and functions of septins and are, therefore, important to eventually incorporate in *in vitro* studies. Protocols for the purification of Borg proteins and anillin have been reported^{54,57}.

The septin purification protocol reported here offers a standardized way to purify septins in their oligomer form with the correct subunit stoichiometry, offering an important advance over many earlier *in vitro* studies relying on single septin subunits. Even though some septins in specific contexts can act as a single subunit², the current body of literature strongly suggests that, in animal cells, septins mostly function in complexes^{9,58}. Therefore, the use of pre-formed hetero-oligomers, such as the ones described in this paper and others^{10,11,18,32,35,36,37}, is of great importance to study the structural and biophysical properties of septins via *in vitro* reconstitution to dissect their functions in the cell. Furthermore, septins are self-assembling proteins with many interaction partners, including the membrane and the cytoskeleton, which makes them of great interest for bottom-up synthetic biology^{59,60,61} and studies of protein-induced changes in membrane biophysical properties such as curvature^{42,62,63}.

Disclosures

The authors declare no competing or financial interests.

Acknowledgments

We thank Cecilia de Agrela Pinto, Tomás de Garay, and Katharina Häußermann for their assistance with mass photometry (iSCAT) experiments; Arjen Jakobi and Wiel Evers for their help with TEM; Lucia Baldauf for her assistance

with TIRF; Pascal Verdier-Pinard for his advice concerning native electrophoresis; Agata Szuba and Marjolein Vinkenoog for their help in setting up the *Drosophila* septin purification efforts, and the Cell and Tissue Imaging (PICT-IBISA), Institut Curie, member of the French National Research Infrastructure France-BioImaging (ANR10-INBS-04). This research received funding from the Netherlands Organization for Scientific Research (NWO/OCW) through the 'BaSyC-Building a Synthetic Cell' Gravitation grant (024.003.019) and from the Agence Nationale pour la Recherche (ANR grants ANR-17-CE13-0014: "SEPTIMORF"; ANR-13-JSV8-0002-01: "SEPTIME"; and ANR-20-CE11-0014-01: "SEPTSCORT").

References

1. Mostowy, S., Cossart, P. Septins: The fourth component of the cytoskeleton. *Nature Reviews Molecular Cell Biology*. **13** (3), 183-194 (2012).
2. Shuman, B., Momany, M. Septins from protists to people. *Frontiers in Cell and Developmental Biology*. **9**, 3802 (2022).
3. Bridges, A. A., Gladfelter, A. S. Septin form and function at the cell cortex. *Journal of Biological Chemistry*. **290** (28), 17173-17180 (2015).
4. Smith, C. et al. Septin 9 exhibits polymorphic binding to F-actin and inhibits myosin and cofilin activity. *Journal of Molecular Biology*. **427** (20), 3273-3284 (2015).
5. Gilden, J. K., Peck, S., Chen, Y. C. M., Krummel, M. F. The septin cytoskeleton facilitates membrane retraction during motility and blebbing. *Journal of Cell Biology*. **196** (1), 103-114 (2012).

6. Marquardt, J., Chen, X., Bi, E. Architecture, remodeling, and functions of the septin cytoskeleton. *Cytoskeleton*. **76** (1), 7-14 (2018).
7. Van Ngo, H., Mostowy, S. Role of septins in microbial infection. *Journal of Cell Science*. **132** (9), jcs226266 (2019).
8. Fung, K. Y. Y., Dai, L., Trimble, W. S. Cell and molecular biology of septins. *International Review of Cell and Molecular Biology*. **310**, 289-339 (2014).
9. Kinoshita, M., Field, C. M., Coughlin, M. L., Straight, A. F., Mitchison, T. J. Self- and actin-templated assembly of mammalian septins. *Developmental Cell*. **3** (6), 791-802 (2002).
10. Iv, F. et al. Insights into animal septins using recombinant human septin octamers 2 with distinct SEPT9 isoforms. *Journal of Cell Science*. **134** (15), jcs258484 (2021).
11. Szuba, A. et al. Membrane binding controls ordered self-assembly of animal septins. *eLife*. **10**, e63349 (2021).
12. Kinoshita, M. Assembly of mammalian septins. *Journal of Biochemistry*. **134** (4), 491-496 (2003).
13. Connolly, D. et al. Septin 9 isoform expression, localization and epigenetic changes during human and mouse breast cancer progression. *Breast Cancer Research*. **13** (4), R76 (2011).
14. Connolly, D. et al. Septin 9 amplification and isoform-specific expression in peritumoral and tumor breast tissue. *Biological Chemistry*. **395** (2), 157-167 (2014).
15. Estey, M. P., Di Ciano-Oliveira, C., Froese, C. D., Bejide, M. T., Trimble, W. S. Distinct roles of septins in cytokinesis: SEPT9 mediates midbody abscission. *Journal of Cell Biology*. **191** (4), 741-749 (2010).
16. John, C. M. et al. The *Caenorhabditis elegans* septin complex is nonpolar. *EMBO Journal*. **26** (14), 3296-3307 (2007).
17. Field, C. M. et al. A purified *Drosophila* septin complex forms filaments and exhibits GTPase activity. *Journal of Cell Biology*. **133** (3), 605-616 (1996).
18. Bertin, A. et al. *Saccharomyces cerevisiae* septins: Supramolecular organization of heterooligomers and the mechanism of filament assembly. *Proceedings of the National Academy of Sciences of the United States of America*. **105** (24), 8274-8279 (2008).
19. Sellin, M. E., Sandblad, L., Stenmark, S., Gullberg, M. Deciphering the rules governing assembly order of mammalian septin complexes. *Molecular Biology of the Cell*. **22** (17), 3152-3164 (2011).
20. Akil, A. et al. Septin 9 induces lipid droplets growth by a phosphatidylinositol-5-phosphate and microtubule-dependent mechanism hijacked by HCV. *Nature Communications*. **7**, 12203 (2016).
21. Tanaka-Takiguchi, Y., Kinoshita, M., Takiguchi, K. Septin-mediated uniform bracing of phospholipid membranes. *Current Biology*. **19** (2), 140-145 (2009).
22. Omrane, M. et al. Septin 9 has two polybasic domains critical to septin filament assembly and Golgi integrity. *iScience*. **13**, 138-153 (2019).
23. Carim, S. C., Kechad, A., Hickson, G. R. X. Animal cell cytokinesis: The rho-dependent actomyosin-anilloseptin contractile ring as a membrane microdomain gathering, compressing, and sorting machine. *Frontiers in Cell and Developmental Biology*. **8**, 575226 (2020).
24. Amine, N. El, Kechad, A., Jananji, S., Hickson, G. R. X. Opposing actions of septins and Sticky on Anillin promote

- the transition from contractile to midbody ring. *Journal of Cell Biology*. **203** (3), 487-504 (2013).
25. Renshaw, M. J., Liu, J., Lavoie, B. D., Wilde, A. Anillin-dependent organization of septin filaments promotes intercellular bridge elongation and Chmp4B targeting to the abscission site. *Open Biology*. **4** (1), 130190 (2014).
 26. Vogt, E. T. et al. The ultrastructural organization of actin and myosin II filaments in the contractile ring: new support for an old model of cytokinesis. *Molecular Biology of the Cell*. **28** (5), 613-623 (2017).
 27. Mavrakakis, M. et al. Septins promote F-actin ring formation by crosslinking actin filaments into curved bundles. *Nature Cell Biology*. **16** (4), 322-334 (2014).
 28. Karasmanis, E. P. et al. A septin double ring controls the spatiotemporal organization of the ESCRT machinery in cytokinetic abscission. *Current Biology*. **29** (13), 2174-2182.e7 (2019).
 29. Hagiwara, A. et al. Submembranous septins as relatively stable components of actin-based membrane skeleton. *Cytoskeleton*. **68** (9), 512-525 (2011).
 30. Calvo, F. et al. Cdc42EP3/BORG2 and septin network enables mechano-transduction and the emergence of cancer-associated fibroblasts. *Cell Reports*. **13** (12), 2699-2714 (2015).
 31. Salameh, J., Cantaloube, I., Benoit, B., Poüs, C., Baillet, A. Cdc42 and its BORG2 and BORG3 effectors control the subcellular localization of septins between actin stress fibers and microtubules. *Current Biology*. **31** (18), 4088-4103.e5 (2021).
 32. Kuzmić, M. et al. Septin-microtubule association via a motif unique to isoform 1 of septin 9 tunes stress fibers. *Journal of Cell Science*. **135** (1), jcs258850 (2022).
 33. Shindo, A. et al. Septin-dependent remodeling of cortical microtubule drives cell reshaping during epithelial wound healing. *Journal of Cell Science*. **131** (12), jcs212647 (2018).
 34. Hu, Q., Nelson, W. J., Spiliotis, E. T. Forchlorfenuron alters mammalian septin assembly, organization, and dynamics. *Journal of Biological Chemistry*. **283** (43), 29563-29571 (2008).
 35. Mavrakakis, M., Tsai, F. C., Koenderink, G. H. Purification of recombinant human and *Drosophila* septin hexamers for TIRF assays of actin-septin filament assembly. *Methods in Cell Biology*. **136**, 199-220 (2016).
 36. Nakos, K., Radler, M. R., Spiliotis, E. T. Septin 2/6/7 complexes tune microtubule plus-end growth and EB1 binding in a concentration- and filament-dependent manner. *Molecular Biology of the Cell*. **30** (23), 2913-2928 (2019).
 37. Kaplan, C. et al. Absolute arrangement of subunits in cytoskeletal septin filaments in cells measured by fluorescence microscopy. *Nano Letters*. **15** (6), 3859-3864 (2015).
 38. Castro, D. K. S. V. et al. A complete compendium of crystal structures for the human SEPT3 subgroup reveals functional plasticity at a specific septin interface. *IUCrJ*. **7** (Pt 3), 462-479 (2020).
 39. Jiao, F., Cannon, K. S., Lin, Y.-C., Gladfelter, A. S., Scheuring, S. The hierarchical assembly of septins revealed by high-speed AFM. *Nature Communications*. **11** (1), 1-13 (2020).
 40. Bertin, A. et al. Phosphatidylinositol-4,5-bisphosphate promotes budding yeast septin filament assembly and

- organization. *Journal of Molecular Biology*. **404** (4), 711-731 (2010).
41. Bridges, A. A., Jentsch, M. S., Oakes, P. W., Occhipinti, P., Gladfelter, A. S. Micron-scale plasma membrane curvature is recognized by the septin cytoskeleton. *Journal of Cell Biology*. **213** (1), 23-32 (2016).
 42. Beber, A. et al. Membrane reshaping by micrometric curvature sensitive septin filaments. *Nature Communications*. **10**, 420 (2019).
 43. Zhou, R., Shi, Y., Yang, G. Expression, purification, and enzymatic characterization of intramembrane proteases. in *Methods in Enzymology*. **584**, 127-155 (2017).
 44. Diebold, M. L., Fribourg, S., Koch, M., Metzger, T., Romier, C. Deciphering correct strategies for multiprotein complex assembly by co-expression: Application to complexes as large as the histone octamer. *Journal of Structural Biology*. **175** (2), 178-188 (2011).
 45. Lebedeva, M. A., Palmieri, E., Kukura, P., Fletcher, S. P. Emergence and rearrangement of dynamic supramolecular aggregates visualized by interferometric scattering microscopy. *ACS Nano*. **14** (9), 11160-11168 (2020).
 46. Ludtke, S. J., Baldwin, P. R., Chiu, W. EMAN: Semiautomated software for high-resolution single-particle reconstructions. *Journal of Structural Biology*. **128** (1), 82-97 (1999).
 47. Zivanov, J. et al. New tools for automated high-resolution cryo-EM structure determination in RELION-3. *eLife*. **7**, e42166 (2018).
 48. Frank, J. et al. SPIDER and WEB: Processing and visualization of images in 3D electron microscopy and related fields. *Journal of Structural Biology*. **116** (1), 190-199 (1996).
 49. Young, G., Kukura, P. Interferometric scattering microscopy. *Annual Review of Physical Chemistry*. **70**, 301-322 (2019).
 50. Young, G. et al. Quantitative mass imaging of single biological macromolecules. *Science*. **360** (6387), 423-427 (2018).
 51. Hernández-Rodríguez, Y., Momany, M. Posttranslational modifications and assembly of septin heteropolymers and higher-order structures. *Current Opinion in Microbiology*. **15** (6), 660-668 (2012).
 52. Ribet, D. et al. SUMOylation of human septins is critical for septin filament bundling and cytokinesis. *Journal of Cell Biology*. **216** (12), 4041-4052 (2017).
 53. Sinha, I. et al. Cyclin-dependent kinases control septin phosphorylation in *Candida albicans* hyphal development. *Developmental Cell*. **13** (3), 421-432 (2007).
 54. Sheffield, P. J. et al. Borg/Septin interactions and the assembly of mammalian septin heterodimers, trimers, and filaments. *Journal of Biological Chemistry*. **278** (5), 3483-3488 (2003).
 55. Joberty, G. et al. Borg proteins control septin organization and are negatively regulated by Cdc42. *Nature Cell Biology*. **3** (10), 861-866 (2001).
 56. Chen, X., Wang, K., Svitkina, T., Bi, E. Critical roles of a RhoGEF-anillin module in septin architectural remodeling during cytokinesis. *Current Biology*. **30** (8), 1477-1490.e3 (2020).

57. Kučera, O. et al. Anillin propels myosin-independent constriction of actin rings. *Nature Communications*. **12** (1), 1-12 (2021).
58. Hsu, S. C. et al. Subunit composition, protein interactions, and structures of the mammalian brain sec6/8 complex and septin filaments. *Neuron*. **20** (6), 1111-1122 (1998).
59. Olivi, L. et al. Towards a synthetic cell cycle. *Nature Communications*. **12** (1), 1-11 (2021).
60. Hürtgen, D., Härtel, T., Murray, S. M., Sourjik, V., Schwille, P. Functional modules of minimal cell division for synthetic biology. *Advanced Biosystems*. **3** (6), e1800315 (2019).
61. Jia, H., Schwille, P. Bottom-up synthetic biology: Reconstitution in space and time. *Current Opinion in Biotechnology*. **60**, 179-187 (2019).
62. Cannon, K. S., Woods, B. L., Crutchley, J. M., Gladfelter, A. S. An amphipathic helix enables septins to sense micrometer-scale membrane curvature. *The Journal of Cell Biology*. **218** (4), 1128-1137 (2019).
63. Lobato-Márquez, D., Mostowy, S. Septins recognize micron-scale membrane curvature. *Journal of Cell Biology*. **213** (1), 5-6 (2016).